This is the accepted manuscript of the article that appeared in final form in **Polymer Testing** 43 : 108-122 (2015), which has been published in final form at https://doi.org/10.1016/j.polymertesting.2015.03.004. © 2015 Elsevier under CC BY-NC-ND license (http://creativecommons.org/licenses/by-nc-nd/4.0/)

ANALYSIS OF A REVERSIBLE FIVE-POINT BENDING CONFIGURATION BASED ON A NOVEL TWO-SENSE SUPPORT

F. Mujika[1], M. Asensio[2],G. Vargas[1], A. Boyano[1], J. De Gracia[1]

[1]Materials+Technologies Group, Department of Mechanical Engineering, Polytechnic University College, University of the Basque Country (UPV/EHU), Plaza de Europa 1, 20018 San Sebastián, Spain

[2]IK4-Ikerlan, Departament of Mechanical Design, Paseo J.M Arizmendiarrieta, Arrasate-Mondragon

e-mail: faustino.mujika@ehu.es, masensio@ikerlan.es

ABSTRACT

A novel two-sense support for flexural tests has been designed and manufactured in Ikerlan. The aim of this support is to do two-sense bending fatigue tests. In order to reduce the displacement corresponding to a given stress, a novel test configuration, named five-point bending is modelled analytically. Basically it is a three-point configuration with two supports at the ends that exert forces in the same sense as the applied load. In this way, it is obtained a partial clamping that can be modelled by concentrated loads. The model has been checked carrying out quasi-static three-point and five-point bending tests at different spans in unidirectional carbon/epoxy composite specimens. Flexural modulus and the out-of-plane shear modulus have been obtained by linear regression in both cases, after having obtained experimentally the stiffness of the system.

Key words: three-point bending, five-point bending, two-sense bending test

INTRODUCTION

Research on fatigue of composite materials is mainly based on studying the degradation of its mechanical properties caused by cyclic loading. Tension-tension and tension-compression are the most accepted fatigue tests by international standards (ASTM D3479) since strain distribution across the specimen is practically uniform and damage develops more or less equally in all layers. Although these tests provide reliable S-N data of the tested material, pure traction loading rarely occurs in real applications.

Bending fatigue tests prove to be an excellent alternative since [1] bending often occurs in in-service loading condition, buckling due to compression is no longer an issue, required forces are much smaller and force and displacement are easy to measure. However, in the case of three-point bending, large deflections can be reached and the specimen might show permanent deflection after a few thousand cycles, which may cause impacts between the indenter and the specimen and alter the measuring data [2]. This problem occurs in the case that the specimen deforms always in the same sense, usually applying the load downwards. In a cycle the specimen changes from the initial undeformed state to the maximum deformed state and it returns to the undeformed state. In this case, the stresses at a fixed point are always of the same sign. If two-sense supports are used, after the return to the undeformed position, the load can be applied upwards in order to get the inverse deformed state. In this case, the sign of stresses at a given point change. Otherwise, if the ends of the specimen are clamped, the maximum stress value for the same displacement is greater than in the simply supported case [3]. Nevertheless, to get a clamped end with null rotation is not possible in a real sense.

In the present study, a two-sense rotating support designed and manufactured in Ikerlan is used for carrying out flexural tests. The initial idea was to apply the support to bidirectional three-point bending tests. Nevertheless, locating two supports at each end of the specimen and applying a central load, partial clamping is obtained. Therefore, the stresses are greater for the same displacement and the problem of great displacements can be avoided. Fig. 1 shows the new configuration proposed, named five-point bending test. There is another five-point configuration that has been used for determining the interlaminar strength of composite laminates [4]. The difference between both configurations is that in the present work there are 4 supports and one load application point. In the other configuration there are 3 supports and 2 points of load application symmetrically located.

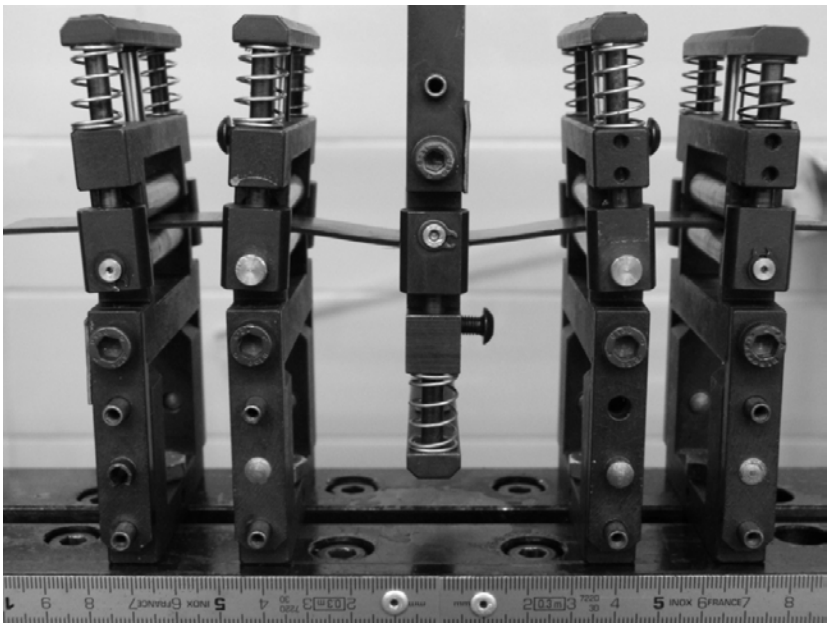

Fig. 1. Five-point bending test configuration with the novel two-sense supports.

The objective of the present work is to describe the novel two-sense supports and to analyze the five-point bending test from a mechanical point of view. This analysis include the bending and shear effects in displacements and the variation of the contact point between the specimen and the support rollers, due to the bending rotations [5]. Three-point and five-point bending tests at different spans have been carried out in order to check the suitability of the proposed method in quasi-static tests, applying the load downwards. In both cases, after having determined the stiffness of the system, the flexural modulus and the out-of-plane shear modulus have been determined by linear regression.

DESCRIPTION OF THE NOVEL SUPPORT

In order to apply the load in both senses, the rotating support shown in Fig. 2 has been designed and manufactured in Ikerlan.

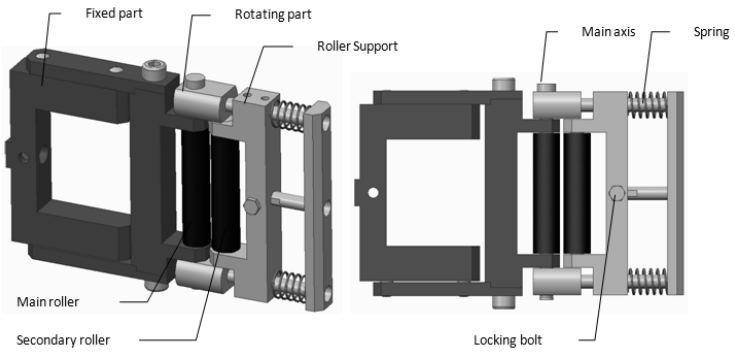

Fig. 2. Two sense rotating support: 3D view and side view

It is divided in two main parts: the fixed one (dark grey), which is attached to the test machine and the rotating one (clear grey), which rotates around the main shaft. Both parts have rollers named main and secondary rollers, which can freely spin around their axes. In the rotating part, the secondary roller and its support are guided allowing the roller to adjust to different specimen thicknesses. The contact between rollers and the specimen is assured by means of two compression springs, dimensioned to avoid indentation. In this way, the supports can be adapted to different sections of the specimen. Once the contact is assured, the support of the secondary roller is fixed by a bolt to the rotating part, avoiding any relative movement during the test. It is worth to underline that the springs do not apply any force once the support is locked. Otherwise, the secondary rollers are able to rotate around the main roller axis. Thus, during bending the rotating part remains perpendicular with respect to the specimen. The rotation of the supports with respect to the mean axes can be appreciated in Fig. 1.

THREE-POINT BENDING TEST

The three-point bending test is analyzed taking into account the effect of span variation and the vertical displacement due to the change of the contact point between the specimen and supports. According to Fig. 1, when the load is downwards the span decreases and when the load is upwards the span increases. The rollers that have contact with the specimen appear in grey in each case.

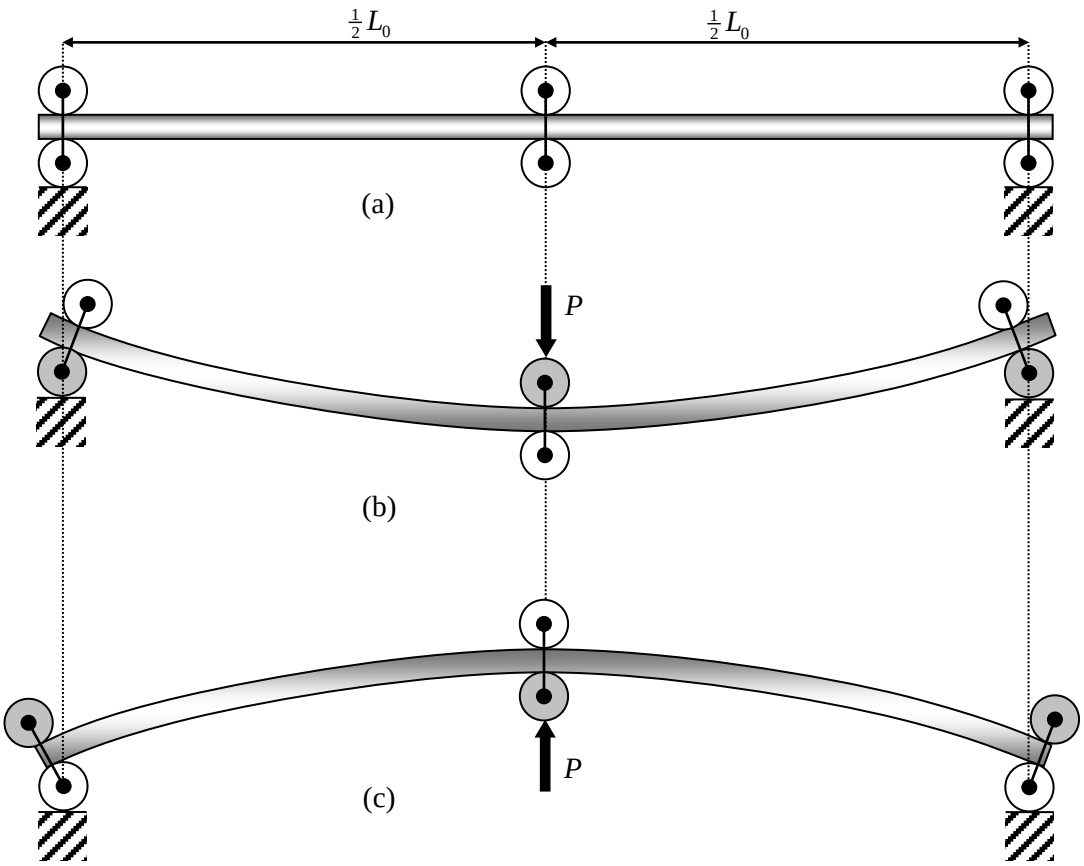

Fig. 3. Three- point bending: (a) Without load; (b) Positive load; (c) Negative load.

When the load is downwards it is defined as positive and when it is upwards it is defined as negative. As the contact point between the specimen and rollers vary due to bending rotation of the specimen, the distances with 0 sub-index in the undeformed configuration change. Variable distances are written without sub-index. The displacement of the specimen is given by [6]:

$$\delta_{sp}^{3p} = \frac{PL^3}{4E_f wh^3} + \frac{3PL}{10Gwh} \tag{1}$$

where E_f is the flexural modulus; $G = G_{13}$ is the out-of-plane shear modulus; I the moment of inertia with respect to the middle plane: $I = \frac{wh^3}{12}$; w the width of the specimen; L is the actual span that includes the change of the contact points; and h is the thickness of the specimen.

There is a vertical displacement component due to the change in the contact point between the roller and the specimen that has not been taken into account up to now. Its effect is of the same order as that concerning span reduction [5]. According to Fig. 4, being C_0 the contact point of the unloaded configuration and C_1 the contact point of the

loaded configuration during the test, the vertical displacement due to the change of the contact point is:

$$\delta_R = R\left(1-\cos\theta\right) \tag{2}$$

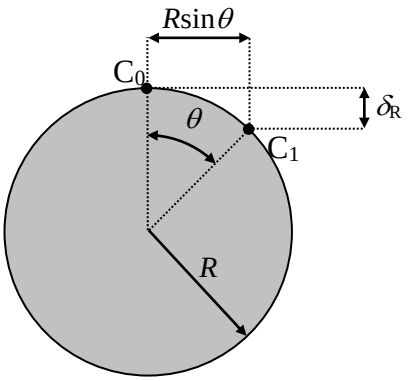

Fig. 4. Horizontal and vertical displacements of the contact point.

According to ISO 14125 [7] standard, bending angles are small when they are lesser than 0.3 rad (17º) [5]. Taking into account the Mclaurin series expansion of the cosine function and considering terms up to second degree, Eq. (2) becomes:

$$\delta_R = \tfrac{1}{2}R\theta^2 \tag{3}$$

Then, without taking into account the stiffness of the testing system, the experimental displacement δ_{3p} is given by :

$$\delta_{3p} = \delta_{sp}^{3p} \pm \tfrac{1}{2}R\theta_{3p}^2 \tag{4}$$

Being δ_{sp} the displacement of the middle point of the specimen and P the load. The sign + corresponds to Fig. 3(b) where the load is positive and the sign – corresponds to Fig. 3(c) where the load is negative. Taking into account the value of θ_{3p}, Eq.(4) can be expresses as:

$$\delta_{3p} = \delta_{sp}^{3p} + \frac{3PL_0^2}{8E_f wh^3}R\left|\theta_{3p}\right| \tag{5}$$

Otherwise, the initial dimensions are considered for the determination of the angle. Eq. (1) can be written as:

$$\delta_{sp}^{3p} = \frac{PL^3}{4E_f wh^3}\left[1+\frac{6}{5}\frac{E_f}{G}\left(\frac{h}{L}\right)^2\right] \tag{6}$$

SPECIMEN CLAMPED AT BOTH ENDS WITH CENTRAL LOAD

The clamped-clamped configuration is assumed as an ideal limit configuration where the bending angles at the ends are null. As the maximum stress for the same displacement at the central point is lesser than in the three-point case, this configuration is more suitable for fatigue tests. Moreover, there are not span variations due to bending angles.

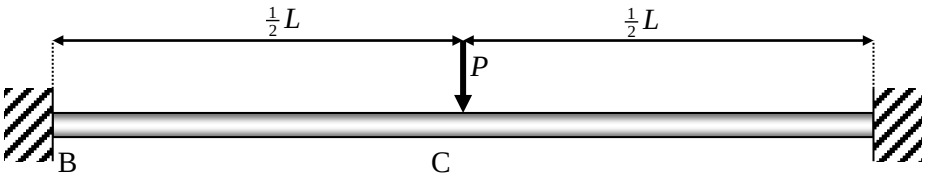

Fig. 5. Clamped-clamped configuration with central load.

Fig. 5 shows the clamped-clamped configuration and Fig. 6 shows one half of the analysed specimen after imposing symmetry conditions. The bending moment in B is adopted as redundant unknown .

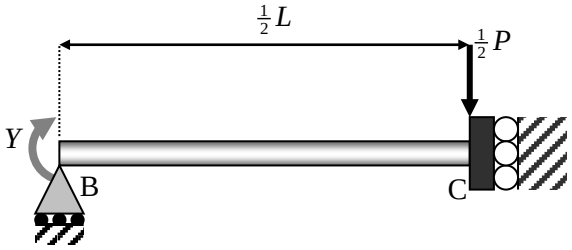

Fig. 6. Unit moment for the determination of *M'* and *V'*.

Shear forces and bending moments in BC are:

$$\begin{aligned} &0 < x_1 < \tfrac{1}{2}L \\ &V = \tfrac{1}{2}P \\ &M = \tfrac{1}{2}Px_1 + Y \end{aligned} \tag{7}$$

The redundant unknown *Y* is determined by applying Engesser-Castigliano's theorem:

$$\int_L \frac{MM'}{E_f I_z} dl + \tfrac{6}{5}\int_L \frac{VV'}{GA} dl = 0 \tag{8}$$

Where *M'* and *V'* are the derivatives with respect to *Y*. After replacing Eq. (7) in Eq (8) and solving it, the redundant unknown is:

$$Y = -\tfrac{1}{8}PL \tag{9}$$

The unit load method is used for obtaining the middle-point displacement in the left half of the system, as depicted in Fig. 7.

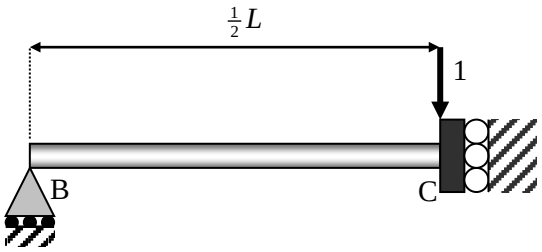

Fig. 7. Load application in the basic system for obtaining *M'* y *V'*.

According to Fig. 4 the derivatives *M'* and *V'* for this system are:

$$\begin{aligned} &0 < x_2 < \tfrac{1}{2}L \\ &V' = 1 \\ &M' = x_2 \end{aligned} \tag{10}$$

The displacement of the middle-point is:

$$\delta_{cc} = \int_L \frac{MM'}{E_f I_z} dl + \tfrac{6}{5}\int_L \frac{VV'}{GA} dl \tag{11}$$

Replacing bending moments and shear forces of Eq. (7) and their derivatives of Eq. (10) in Eq. (11):

$$\delta_{cc} = \frac{PL^3}{16E_f wh^3} + \frac{3PL}{10Gwh} \tag{12}$$

Eq. (12) can be written as:

$$\delta_{cc} = \frac{PL^3}{16E_f wh^3}\left[1 + \frac{24}{5}\frac{E}{G}\left(\frac{h}{L}\right)^2\right] \tag{13}$$

Comparing Eqs. (6) and (13), the relative influence of shear is 4 times greater in the clamped-clamped configuration that in the case of three-point bending.

NEW TEST CONFIGURATION: FIVE-POINT BENDING

Redundant force

As to get total clamping is not possible in a real sense, partial clamping is generated by the use of two sets of two-sense supports. Fig. 8 shows the undeformed test

configuration and the deformed configurations for positive and negative loads, respectively. The rollers that contact with the specimen in each case are in grey.

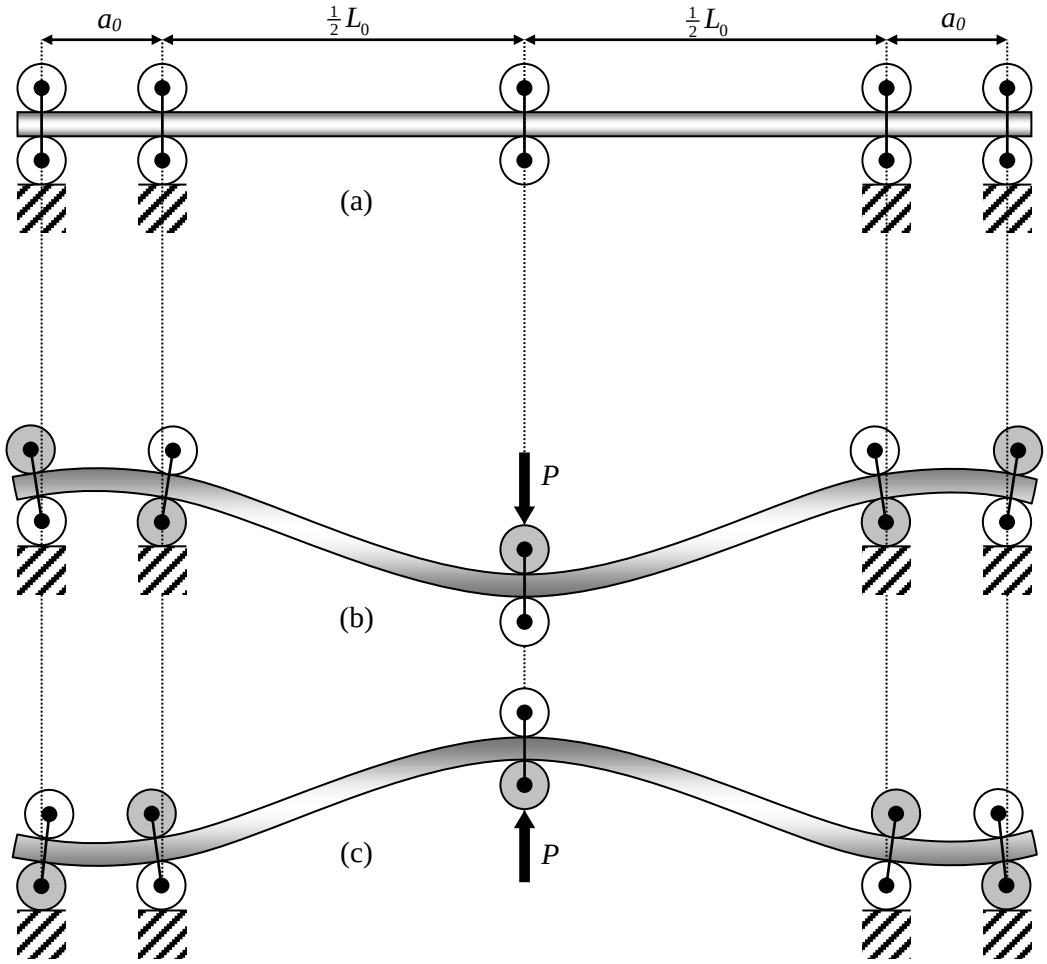

Fig. 8. Five-point bending: (a) Without load; (b) Positive load; (c) Negative load.

.

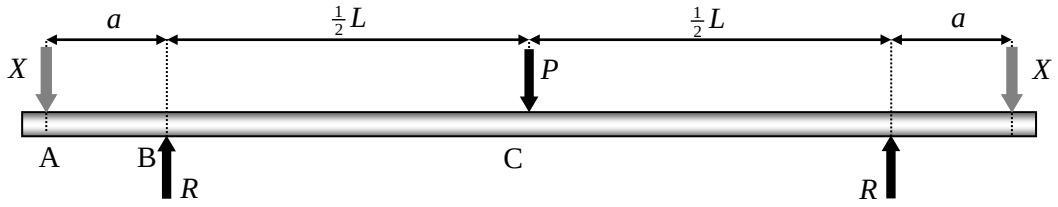

Fig. 9. Applied load and roller reactions for a positive load.

Fig. 9 shows the applied load and reactions, assuming the symmetry of the system and taking as redundant unknown the reaction force at the extreme supports. Fig. 10 shows a half of the system with the corresponding boundary symmetry conditions.

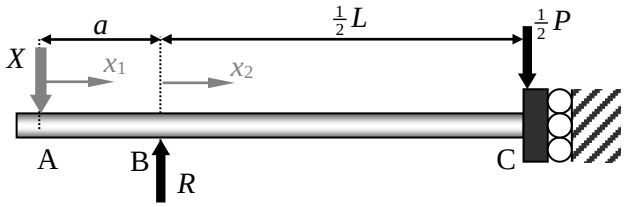

Fig. 10. Left half of the system with boundary symmetry conditions considered for calculations.

Shear forces and bending moments in AB are:

$$\begin{aligned} &0 < x_1 < a \\ &V = -X \\ &M = -Xx_1 \end{aligned} \tag{14}$$

In BC:

$$\begin{aligned} &0 < x_2 < \tfrac{1}{2}L \\ &V = \tfrac{1}{2}P \\ &M = -Xa + \tfrac{1}{2}Px_2 \end{aligned} \tag{15}$$

The redundant unknown X is obtained by the Engesser-Castigliano theorem of Eq. (8). In this case, M' and V' are the derivatives with respect to the force X. Replacing Eqs. (14) and (15) in Eq. (8) and after solving it the redundant unknown is:

$$X = \tfrac{3}{8}P\frac{L^2}{2a^2 + 3aL + \frac{3}{5}\frac{E}{G}h^2} \tag{16}$$

Bending angles at support rollers

The bending angles at supports A and B have influence in the distance variations among the supports during the test. In order to obtain the derivatives of moments and shear forces, unit moments are applied at A and B. In spite of Fig. 11 shows moments applied at both sections, they have to be applied separately. The derivatives of shear forces are null and then, the effect of shear in bending angles is null.

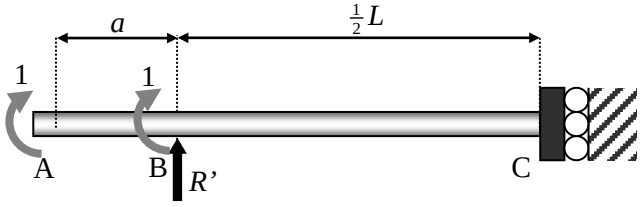

Fig. 11. Unit moments for the determination of M' and V'.

After determining the derivatives, by using the moments of Eqs. (14) and (15), the bending angles at A and B are:

$$\theta_A = \frac{PL^2}{4Ewh^3}\left[1-8\frac{X}{P}\frac{a}{L^2}(a+L)\right]$$
$$\theta_B = \frac{PL^2}{4Ewh^3}\left[1-8\frac{X}{P}\frac{a}{L}\right] \quad (17)$$

As unit moments have been applied clockwise, if the resulting bending angle is positive it is clockwise, and if it is negative it is counter clockwise.

Displacement of the middle-point

Fig. 12 shows a half of the system with a unit load at the middle-point, which is used for applying the unit load method.

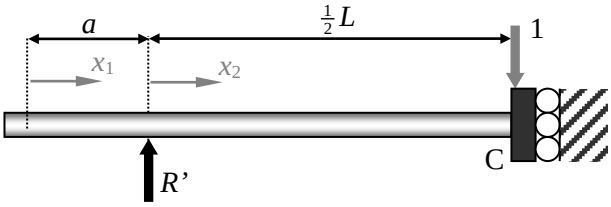

Fig. 12. Application of a unit load in the basic system for obtaining *M'* and *V'*.

M' and *V'* are:

$$0 < x_2 < \tfrac{1}{2}L$$
$$V' = \tfrac{1}{2} \quad (18)$$
$$M' = \tfrac{1}{2}x_2$$

Replacing bending moments and shear forces of Eqs. (14) and (15) and their derivatives of Eq. (18) in Engesser-Castigliano's theorem, the displacement of the specimen at the middle point is:

$$\delta_{sp}^{5p} = \frac{PL^3}{4E_f wh^3} + \frac{3PL}{10Gwh} - \frac{3XaL^2}{2E_f wh^3} \quad (19)$$

The difference between Eq. (19) and Eq. (1) is the term related to the force *X*. Then, three-point bending can be considered as a particular case of five-point bending where $X = 0$. The experimental displacement of the middle point is:

$$\delta_{ex}^{5p} = \delta_{sp}^{5p} \pm R_B \frac{\theta_B^2}{2} \quad (20)$$

The term concerning θ_B is related to the vertical displacement of the contact point, in analogous manner as in Eq. (4) concerning three-point bending.

Length variations

As explained previously, there are length variations related to bending rotations of the specimen. The load can be positive or negative and the displacement of the central point has the same sign than the applied load.

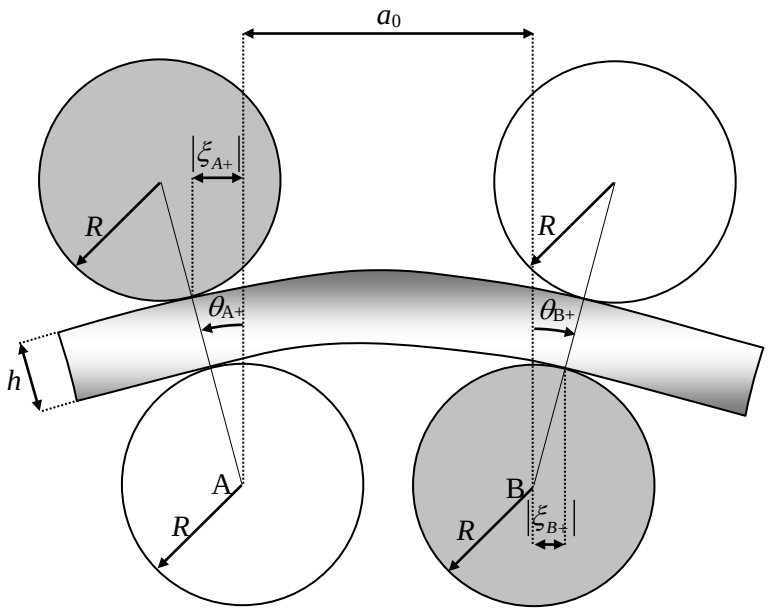

Fig. 13. Length variations between A and B when the load is positive.

The rollers of the left part of the deformed configuration when the load is positive are depicted in Fig. 13. The radius of the support rollers is *R*. Taking into account the Mclaurin series expansion of the sine function and considering terms up to second degree as mentioned above in the case of cosine, it results that $\sin\theta = \theta$. Then, the variations of contact length concerning A and B rollers are:

$$\begin{aligned} |\xi_{A+}| &= |\theta_{A+}|(R+h) \\ |\xi_{B+}| &= |\theta_{B+}|R \end{aligned} \tag{21}$$

Thus, the modified distances taking into account the sign of the angles are:

$$\begin{aligned} a &= a_0 + |\xi_{A+}| + |\xi_{B+}| = a_0 + \xi_{B+} - \xi_{A+} \\ L &= L_0 - 2|\xi_{B+}| = L_0 - 2\xi_{B+} \end{aligned} \tag{22}$$

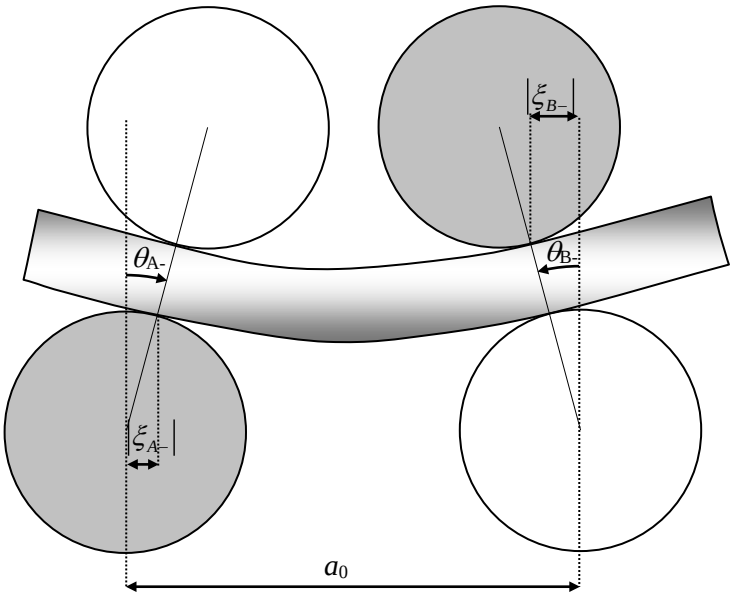

Fig. 14. Length variations between A and B when the load is negative.

According to Fig. 14, the contact length variation when the load is negative are:

$$\begin{aligned} |\xi_{A-}| &= |\theta_{A-}| R \\ |\xi_{B-}| &= |\theta_{B-}| (R+h) \end{aligned} \tag{23}$$

The modified dimensions, taking into account the signs of the angles are:

$$\begin{aligned} a &= a_0 - |\xi_{A-}| - |\xi_{B-}| = a_0 + \xi_{B-} - \xi_{A-} \\ L &= L_0 + 2|\xi_{B-}| = L_0 - 2\xi_{B-} \end{aligned} \tag{24}$$

As the expressions for a and L in Eqs. (22) and (24) are similar, they can be written for both cases as:

$$\begin{aligned} a &= a_0 (1+\eta_a) \qquad \eta_a = \frac{\xi_B - \xi_A}{a_0} \\ L &= L_0 (1-\eta_L) \qquad \eta_L = \frac{2\xi_B}{L_0} \end{aligned} \tag{25}$$

In spite of in Eq. (25) the difference in load sign is not considered, according to Eqs. (21) and (23) ξ parameters vary with the thickness h depending on the load sign. Then, it has to be taken into account that the small adimensional parameters η_a and η_L depend on the load sign. Otherwise, terms of second order or greater related to parameters η will be neglected. Replacing the values of L and a of Eq. (25) in Eq. (16), the force X can be expressed as:

$$X = \tfrac{3}{8} P \frac{L_0^2}{2a_0^2 + 3a_0 L_0 + \tfrac{3}{5}\tfrac{E}{G} h^2}\left(1-\eta_X\right) \qquad \eta_X = 2\eta_L + \frac{4a_0^2\eta_A + 3a_0 L_0\left(\eta_A - \eta_L\right)}{2a_0^2 + 3a_0 L_0 + \tfrac{3}{5}\tfrac{E}{G} h^2} \quad (26)$$

By replacing Eq. (25) in Eq. (19) the middle point displacement is:

$$\delta_{sp}^{5p} = \frac{PL_0^3}{4Ewh^3}\left(1-3\eta_L\right) - \frac{3Pfa_0 L_0^2}{2Ewh^3}\left(1-\eta_c\right) + \frac{3PL_0}{10Gwh}\left(1-\eta_L\right) \quad (27)$$
$$\eta_c = \eta_X + 2\eta_L - \eta_a$$

Where the ratio between the applied load and the redundant force considering initial dimensions is :

$$f = \frac{X_0}{P} = \frac{3}{8}\frac{L_0^2}{2a_0^2 + 3a_0 L_0 + \tfrac{3}{5}\tfrac{E}{G} h^2} = \frac{3}{8}\left(2\alpha + 3\alpha + \tfrac{3}{5}\tfrac{E}{G}\left(\tfrac{h}{L_0}\right)^2\right)^{-1} \quad (28)$$

where $\alpha = \dfrac{a_0}{L_0}$

Considering two different points at the same test, the variation of displacement is:

$$\left(\delta_{sp}^{5p}\right)_2 - \left(\delta_{sp}^{5p}\right)_1 = \left(P_2 - P_1\right)\left\{\begin{array}{l} \dfrac{L_0^3}{4Ebh^3}\left[1-3\left(\eta_{L1}+\eta_{L2}\right)\right] - \dfrac{3fa_0 L_0^2}{2Ebh^3}\left[1-\left(\eta_{c1}+\eta_{c2}\right)\right] \\ + \dfrac{3L_0}{10Gbh}\left[1-\left(\eta_{L1}+\eta_{L2}\right)\right] \end{array}\right\} \quad (29)$$

As the experimental displacement includes also the vertical displacement of the contact point, according to Eq. (20) and replacing the value of given in Eq. (17) it results:

$$\left(\delta_{ex}^{5p}\right)_2 - \left(\delta_{ex}^{5p}\right)_1 = \left(\delta_{sp}^{5p}\right)_2 - \left(\delta_{sp}^{5p}\right)_1 \pm \left(P_2 - P_1\right)\frac{L_0^2}{8E_f bh^3}\left(1-8\alpha f\right)R\left(\theta_{B1}+\theta_{B2}\right) \quad (30)$$

Combining Eq. (29) and Eq. (30)

$$\Delta\delta_{ex}^{5p} = \Delta P\left\{\begin{array}{l} \dfrac{L_0^3}{4Ebh^3}\left(1-3\eta_{L(1+2)}\right) + \dfrac{L_0^2}{8Ebh^3}\left[-12\,fa_0\left(1-\eta_{c(1+2)}\right) \pm \left(1-8\alpha f\right)R\theta_{B(1+2)}\right] \\ + \dfrac{3L_0}{10Gbh}\left[1-\eta_{L(1+2)}\right] \end{array}\right\} \quad (31)$$

where the following condensed nomenclature has been used for the correction terms: $\eta_{L(1+2)} = \eta_{L1} + \eta_{L2}$, and so on.

As the angle θ_B has the same sign that the load, the ± sign can be modified by a + sign, using the absolute value of the angle:

$$\Delta\delta_{ex}^{5p} = \Delta P \left\{ \begin{array}{l} \dfrac{L_0^3}{4Ebh^3}\left(1-3\eta_{L(1+2)}\right)+\dfrac{L_0^2}{8Ebh^3}\left[-12\,fa_0\left(1-\eta_{c(1+2)}\right)+\left(1-8\alpha f\right)R\left|\theta_{B(1+2)}\right|\right] \\ +\dfrac{3L_0}{10Gbh}\left[1-\eta_{L(1+2)}\right] \end{array} \right\} \quad (32)$$

Being $m = \dfrac{\Delta P}{\Delta\delta_{ex}^{5p}}$ the slope of the load-displacement curve, the bending modulus is:

$$E_f = \frac{mL_0^3}{4wh^3}\left\{ \begin{array}{l} \left(1-3\eta_{L(1+2)}\right)+\dfrac{1}{2L_0}\left[-12\,fa_0\left(1-\eta_{c(1+2)}\right)+\left(1-8\alpha f\right)R\left|\theta_{B(1+2)}\right|\right] \\ +\dfrac{6}{5}\dfrac{E}{G}\left(\dfrac{h}{L}\right)^2\left(1-\eta_{L(1+2)}\right) \end{array} \right\} \quad (33)$$

Otherwise, the maximum strain is located at the middle of the specimen, where the moment is maximum, being

$$\varepsilon_{5p} = \frac{6PL_0}{E_f wh^2}\frac{4\alpha+3+2\phi}{8\left(2\alpha+3+\phi\right)} \quad (34)$$

where $\phi = \dfrac{3}{5\alpha}\dfrac{E_f}{G}\left(\dfrac{h}{L_0}\right)^2$

Three-point bending as a particular case of five-point bending

As three-point bending can be considered as a particular case of five-point bending when $X = 0$, the bending modulus in three-point flexure can be determined from Eq. (33) with $f = 0$ as:

$$E_f = \frac{mL_0^3}{4wh^3}\left\{\left(1-3\eta_{L(1+2)}\right)+\frac{1}{2L_0}\left[R\left|\theta_{B(1+2)}\right|\right]+\frac{6}{5}\frac{E}{G}\left(\frac{h}{L}\right)^2\left(1-\eta_{L(1+2)}\right)\right\} \quad (35)$$

In the case that the load is positive, the modulus in 3-point bending is given by:

$$E_f = \frac{mL_0^3}{4wh^3}\left\{\left(1-2.25\frac{R}{h}\varepsilon_{3p(1+2)}\right)+\frac{6}{5}\frac{E}{G}\left(\frac{h}{L}\right)^2\left(1-\frac{R}{h}\varepsilon_{3p(1+2)}\right)\right\} \quad (36)$$

where ε_{3p} is the maximum strain in three-point bending given by:

$$\varepsilon_{3p} = \frac{3PL_0}{2E_f wh^2} \quad (37)$$

Diagrams of bending moments

Fig. 15 shows the three configurations previously analyzed and the diagrams of bending moments normalized with respect to (*PL*). The maximum normalized moment occurs in three-point bending. In the case of the clamped-clamped beam the bending moments are the same at the clamped ends and at the central section. However, the moment *fa* at the support in five-point bending is lesser than that of the middle section. Therefore, the maximum stress zone in five-point bending is localized in the middle of the specimen, as in three-point bending. This is a positive aspect of the five-point configuration. In spite of the normalized moment for a given load *P* at the centre is lesser in five-point bending than in three-point bending , the displacement is greater in three-point bending.

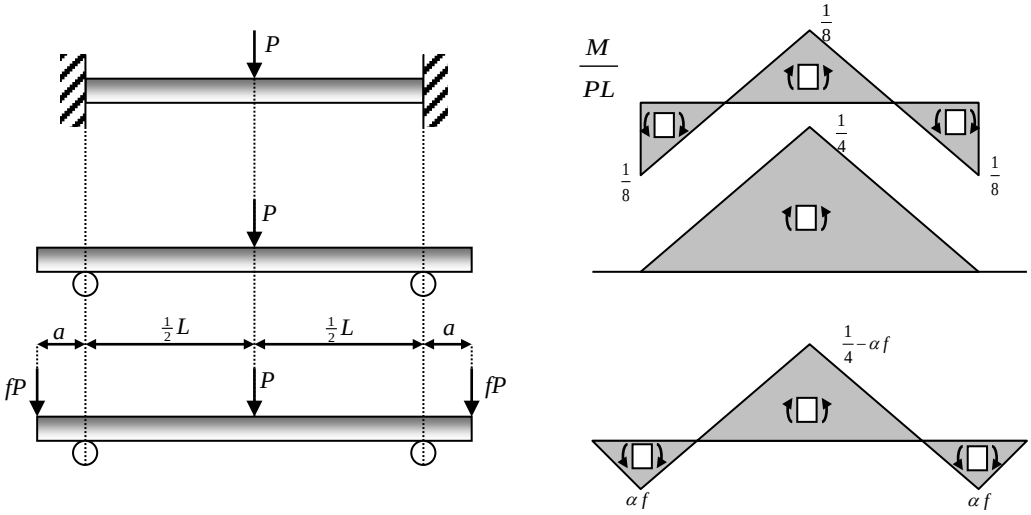

Fig. 15. Bending moment diagrams for the three configurations.

Strain-displacement ratio

In fatigue tests it is desirable to obtain a great ratio between the maximum strain and the maximum displacement in order to obtain a great value of stress for the same displacement. In order to determine the mentioned ratio, only bending effects are considered. Maximum strain corresponding to the maximum bending moment is:

$$\varepsilon_{\max} = \frac{6M_{\max}}{Ewh^2} \tag{38}$$

Table 1 shows the ratios between the maximum strain and the maximum displacement, which only depends on the geometry of the test. The effect of distance variations between supports is not considered. The ratio in the clamped-clamped case is twice the

ratio in three-point bending. Then, for the same displacement the stress is twice. In five-point bending the ratio depends on the parameter α.

Table 1. Ratio between maximum strain and maximum displacement due to bending.

	$\frac{\varepsilon_{max}}{\delta_{max}}$
Clamped-clamped	$12\frac{h}{L^2}$
three-point bending	$6\frac{h}{L^2}$
five-point bending	$12\frac{h}{L^2}\frac{3+4\alpha}{3+8\alpha}$

Fig. 16 shows the clamping degree, defined as the ratio between values that correspond to the clamped-clamped case and to five-point bending, respectively, being: $\frac{3+4\alpha}{3+8\alpha}$. When the parameter α varies between 0.1 and 1, the clamping degree varies between 89% and 64%.

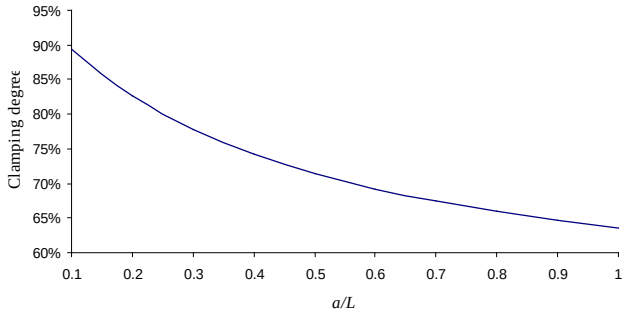

Fig. 16. Clamping degree as a function of the ratio $\alpha = a/L$.

Shear forces

In five-point bending, the shear forces between support rollers that conform the partial clamping depend on α parameter. In the case of unidirectional composites those forces could lead to delamination of the specimen at these zones. Without taking into account the term due to shear, the parameter *f* given in Eq. (28) and only depends on α, being:

$$f = \frac{X_0}{P} = \frac{3}{8}\frac{1}{2\alpha^2 + 3\alpha} \tag{39}$$

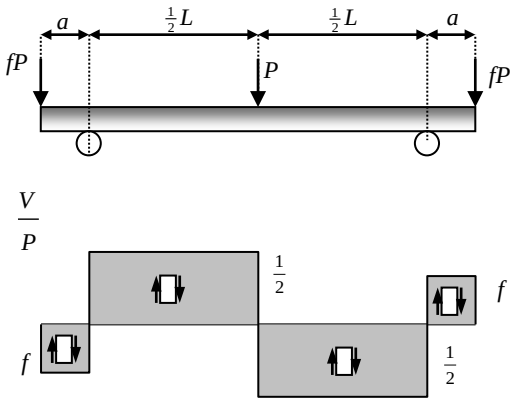

Fig. 17. Diagram of shear forces in five-point bending.

Fig. 17 shows the diagram of shear forces in five-point bending. Fig. 18 shows the variation of f with respect to α for the same range considered in Fig. 16. Then, in order to get shear forces lesser than 0.5 P in the zone between rollers the ratio α must be $\alpha >$ 0.22.

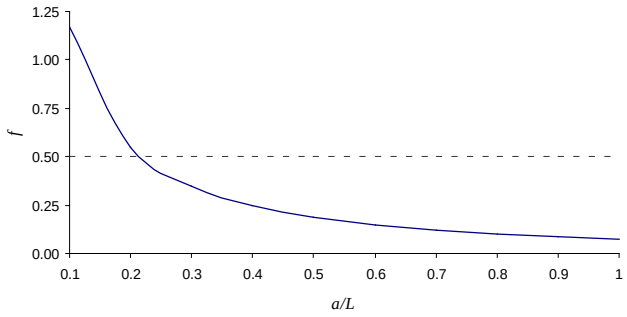

Fig. 18. Shear force factor as a function of the ratio $\alpha = a/L$.

DETERMINATION OF FLEXURAL MODULUS

Three-point bending

In three-point bending, according to Eq. (36) the flexural modulus can be expressed as:

$$E_f = \frac{mL_0^3}{4wh^3}\beta_{3pc}\left\{1 + 1.2\frac{E_f}{G_{13}\beta_{3p}}\left(\frac{h}{L}\right)^2\left(1 - \frac{R}{h}\varepsilon_{3p(1+2)}\right)\right\}$$
$$\beta_{3pc} = \left(1 - 2.25\frac{R}{h}\varepsilon_{3p(1+2)}\right) \tag{40}$$

Eq.(40) can be written as

$$E_{3pc}^{-1} = E_f^{-1}\left\{1+1.2\frac{E_f}{G_{13}\beta_{3p}}\left(\frac{h}{L}\right)^2\left(1-\frac{R}{h}\varepsilon_{3p(1+2)}\right)\right\}$$
$$E_{3pc} = \frac{mL_0^3}{4wh^3}\beta_{3pc} \tag{41}$$

Where E_{3pc} is the usual expression of the flexural modulus corrected by the effect of the change of the contact point on the supports. Then, the following linear relation can be written

$$E_{3pc}^{-1} = A + Bx$$
$$x = \frac{1.2}{\beta_{3pc}}\left(\frac{h}{L}\right)^2\left(1-\frac{R}{h}\varepsilon_{3p(1+2)}\right) \tag{42}$$
$$E_f = A^{-1} \quad G = B^{-1}$$

After determining E_{3pc} in the same specimen for different spans, E_f and G can be determined by linear regression from Eqs. (42). If the same strain range is used in all cases, Eq. (42) can be written as:

$$E_{3p}^{-1} = A + Bx$$
$$x = \left(\frac{h}{L}\right)^2 \quad E_{3p} = \frac{mL_0^3}{4wh^3} \tag{43}$$
$$E_f = \left(1-2.25\frac{R}{h}\varepsilon_{3p(1+2)}\right)A^{-1} \quad G = 1.2\left(1-\frac{R}{h}\varepsilon_{3p(1+2)}\right)B^{-1}$$

Five-point bending

E_f can be obtained from Eq.(33) as:

$$E_f = \frac{mL_0^3}{4bh^3}\left\{\begin{array}{l}\left(1-3\eta_{L(1+2)}\right)+\dfrac{1}{2L_0}\left[-12\,fa_0\left(1-\eta_{c(1+2)}\right)+\left(1-8\alpha f\right)R\left|\theta_{B(1+2)}\right|\right] \\ +\dfrac{6}{5}\dfrac{E_f}{G}\left(\dfrac{h}{L}\right)^2\left(1-\eta_{L(1+2)}\right)\end{array}\right\} \tag{44}$$

Grouping the terms related to bending in a parameter β, Eq. (44) can be written as:

$$E_f = \frac{mL_0^3}{4wh^3}\beta_{5pc}\left\{1+\frac{6}{5}\frac{E}{G\beta_{5p}}\left(\frac{h}{L}\right)^2\left(1-\eta_{L(1+2)}\right)\right\}$$
$$\beta_{5pc} = \left(1-3\eta_{L(1+2)}\right)+\frac{1}{2L_0}\left[-12\,fa_0\left(1-\eta_{c(1+2)}\right)+\left(1-8\alpha f\right)R\left|\theta_{B(1+2)}\right|\right] \tag{45}$$

where the sub-index *c* indicates that corrections are included. Eq. (45) can be written in the form

$$E_{5pc}^{-1} = E_f^{-1}\left\{1+\frac{6}{5}\frac{E_f}{G\beta_{5p}}\left(\frac{h}{L}\right)^2\left(1-\eta_{L(1+2)}\right)\right\}$$
$$E_{5pc} = \frac{mL_0^3}{4wh^3}\beta_{5pc} \tag{46}$$

From Eq. (46) the following linear relation can be written as:

$$E_{5pc}^{-1} = C + Dx$$
$$x = 1.2\left(\frac{h}{L}\right)^2\frac{\left(1-\eta_{L(1+2)}\right)}{\beta} \tag{47}$$
$$E_f = A^{-1} \quad G = B^{-1}$$

After determining E_{5pc} in the same specimen for different spans, E_f and G can be determined by linear regression from Eqs. (47).

In five-point bending the rotated angles are lesser than in three-point bending. If the correction terms are considered negligible, Eq. (47) becomes in:

$$E_{5p}^{-1} = C + Dx$$
$$x = \frac{1.2}{\beta_{5p}}\left(\frac{h}{L}\right)^2 \quad E_{5p} = \frac{mL_0^3}{4wh^3}\beta_{5p} \quad \beta_{5p} = 1-6f\alpha \tag{48}$$
$$C = E_f^{-1} \quad D = G^{-1}$$

EXPERIMENTAL

Material, tests and apparatus

Three specimens of T6T/F593 unidirectional carbon/epoxy from Hexcel Composites with 50% fiber volume content were used for experiments. Three-point and five-point bending tests were carried out at different spans using an electromechanical testing machine Tinius Olsen H300KU updated by Zwick/Roell. A 10kN load cell was used.

The radius of the support cylinders was R=5mm and the spans used were (mm): 40, 48, 60, 80 and 120. Three tests were carried out for each condition. The slopes of the load-displacement curves were obtained for a fixed strain range between 0.25% and 0.45%. For this purpose, strains have to be determined during the test. If the calculation is carried out based on displacement data, the effect of local deformation and shear need to be included, but they are not known. Thus, strains were determined based on the measurement of loads according to Eqs. (37) and (34), for three-point and five-point tests, respectively, with approximate values of E_f and G.

Stiffness of the testing system

If the displacement of the specimen is determined by the displacement of the load application, the stiffness of the system k_{sys} must be determined. It can be done by and indentation test, determining the stiffness in a linear zone of the load-displacement curve [6]. Then, the primary displacement δ_{pri} measured by the machine can be corrected during the test subtracting the displacement due to the testing system for obtaining the experimental displacement $\delta_{\exp}$:

$$\delta_{\exp} = \delta_{\text{pri}} - C_{sys} P \tag{49}$$

Where $C_{sys} = k_{sys}^{-1}$ is the compliance of the system. Other way for including the compliance of the system is to consider the system and the specimen as two linear springs subjected to the same load P, as depicted in Figure Fig. 19.

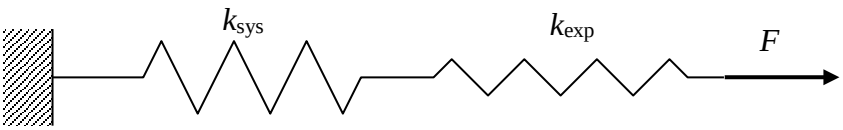

Fig. 19. Experimental stiffness and system stiffnesses

As the experimental displacement is the sum of the displacements of the specimen and the load, the relation between compliances is:

$$C_{\exp} = C_{pri} - C_{sys} \tag{50}$$

The stiffness of the system includes all aspects away of the stiffness of the specimen: Testing fixture, load cell, testing machine structure and the local deformability of the specimen. This effects has been named also "local deformation effect" [6]. Otherwise, Fig. 20 shows the elastic supports assumed in the case of a five-point bending test.

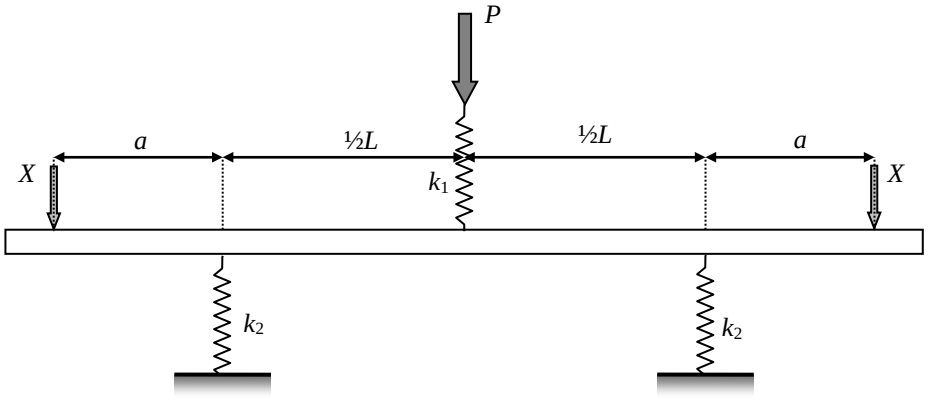

Fig. 20. Elastic supports considered in five-point bending

k_1 is the stiffness corresponding to the testing system, the load application support and the local deformation of the specimen. k_2 is the stiffness corresponding to the lower supports. k_{sys} is the stiffness of the global system. The respective compliances are named as C_i. The stiffness of the outer support is not considered, as the force is applied in the opposite sense with respect to the other supports. Due to the difficulty of measuring this stiffness, it is assumed to be infinite in a first approach.

Considering a rigid specimen, the relation between displacements, as a function of the compliances is:

$$PC_{sys} = \left(\tfrac{1}{2}P + X\right)C_2 + PC_1 \tag{51}$$

According to Eq. (28), Eq. (51) can be written as:

$$C_{sys} = \left(\tfrac{1}{2} + f\right)C_2 + C_1 \tag{52}$$

Thus, C_{sys} depends on the value of f and it depends on the span used, according to Eq. (28). In three point bending $f = 0$ and thus

$$C_{sys} = \tfrac{1}{2}C_2 + C_1 \tag{53}$$

C_1 can be determined by an indentation test carried out with a rigid basis, as shown in Fig. 21a. Otherwise, C_{sys} can be determined in three-point bending with the specimen on a rigid basis supported at lower supports, as shown in Fig. 21b.

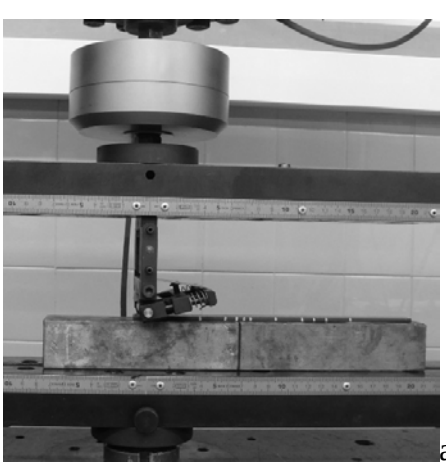
a/


b/

Fig. 21. Test for determining different stiffnesses: a/ Determination of k_1; b/ Determination of k_s

Extracting C_2 from Eq. (53) it results

$$C_2 = 2\left(C_{sys} - C_1\right) \tag{54}$$

Having obtained C_2 by three-point bending, C_{sys} in five-point bending can be obtained in each case from Eq (52). The experiments shown in Fig. 21 have been carried out up to 3000 N in order to prevent damage the supports. The stiffnesses have been obtained in the range 2000-3000 N being

$$k_{sys} = 9800 \text{ N/mm}; \; k_1 = 11600 \text{ N/mm}$$

Displacement rate

The displacement rate was varied according to ISO 14125[7] in order to get a constant strain rate of 0.01min^{-1}. Taking into account that displacement depend on shear and local deformation, these effects should be included. The ratio between the displacement and the strain is obtained from Eqs. (6) and (37) in the case of three-point bending and from Eqs. (19) and (34) in the case of five-point bending. Without considering corrections terms related to the change of the contact point, the displacement rate in each case was calculated according to

$$\begin{aligned} \dot{\delta}_{3p} &= \frac{L_0^2}{6h}\dot{\varepsilon}\left[1+1.2\frac{E_f}{G}\left(\frac{h}{L_0}\right)^2+4\frac{E_f b}{k_s}\left(\frac{h}{L_0}\right)^3\right] \\ \dot{\delta}_{5p} &= \frac{L_0^2}{12h}\frac{8\alpha+3+4\eta}{4\alpha+3+2\eta}\dot{\varepsilon}\left[1+1.2\frac{E_f}{G\beta_{5p}}\left(\frac{h}{L_0}\right)^2+4\frac{E_f b}{k_s\beta_{5p}}\left(\frac{h}{L_0}\right)^3\right] \end{aligned} \tag{55}$$

where k_{sys} = 10000 N/mm has been adopted as the stiffness of the system in both cases.

Preliminary results

In each specimen, three-point tests have been carried out with L_0 = 200 mm. This span is considered great enough for neglecting shear and local deformation effects. Table 1 shows the dimensions and the flexural modulus of the specimens.

Table 2. Dimension and flexural modulus of the specimens

	b (mm)	h (mm)	L_0(mm)	E_f (GPa)
S1	15.4	3.02	200	106.5
S2	15.2	3.03	200	104.4
S3	15	3.03	200	105.3

According to Table 1, the approximate value of modulus for determining strains has been E_f = 105 GPa. With respect to the value of G needed in the case of five-point bending, it has been considered G = 4 GPa [6].

The same specimens have been also tested in three-point bending in a MTS machine for the same spans, with usual bending supports. The stiffness of the system was k_s = 24000 N/mm. The results obtained are shown in Table 3.

Table 3. Values obtained with usual bending supports

	S1	S2	S3
E_f(GPa)	106.6	103.7	104.2
G (Mpa)	3.8	4.3	4.6

The differences between the flexural modulus E_f shown in Table 2 and Table 3 are below 1% for each specimen.

Influence of shear and system stiffness with respect to bending

The summands into brackets in Eq. (55) show the influence of shear and stiffness with respect to bending. Fig. 22 shows the comparison of those influences in three-point and five-point bending, assuming the following nominal properties and dimensions:

E_f = 105.0 GPa; G = 4.0 GPa; k_s = 10 kN/mm; a = 40 mm, h = 3 mm; b = 15 mm

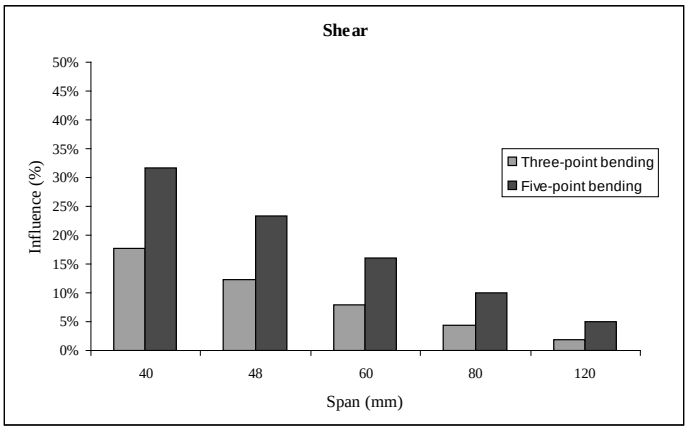

(a)

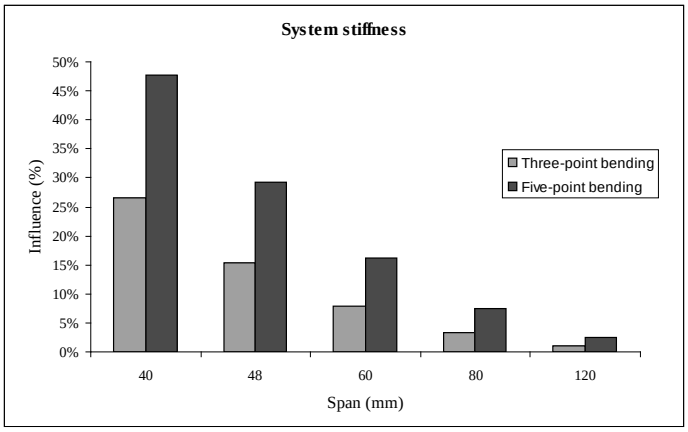

(b)

Fig. 22. Influence of shear and stiffnes with respect to bending: a/ Shear influence. b/ System stiffness

According to Fig. 21, the influence of shear and system stiffness is more important in the case of five-point bending than in three-point bending. Otherwise, according to Eq. (55) the ratio between influences in both tests is the same. In both tests the influence of system stiffness is greater than the influence of shear for spans of 40 and 48 mm. For the span of 60 mm the influences are equal. For spans of 80 mm and 120 mm, the influence of shear is greater than the influence of system stiffness.

Regression results for three-point and five-point bending

It has been observed that in both cases the influence of the system stiffness is very important. In particular, in three-point bending, to use k_s = 9800 N/mm lead to G values to be too great. Then, it has been assumed that in three-point bending the lower supports are rigid and thus k_s = 11600 N/mm has been considered. This assumption is related to the fact that in the determination of k_s shown in Fig. 21 the forces on the lower supports are vertical, in the same direction that the support. In three-point bending, the variation of the contact point is more pronounced that in the case of five-point bending. Thus, the load on the lower support does not act along the symmetry plane. As a consequence, the support is considered rigid in three-point bending as a first approach.

Table 4 shows the results obtained by linear regression for five spans in the case of five-point bending and for 6 span in the case of three-point bending, as the values corresponding to the span of 200 mm given in Table 2 have been also included.

Table 4. Experimental results obtained by linear regression in three-point and five-point tests

	S1	S2	S3

	3P	5P	3P	5P	3P	5P
E_f (GPa)	105.7	104.3	103.5	101.8	104.6	102.5
G (GPa)	4.1	4.1	3.8	3.9	3.8	4.1
R^2	0.958	0.981	0.958	0.981	0.973	0.987

The results of E_f in Table 4 obtained by three-point and five-point bending agree well between them and agree also with values of Table 3 obtained in other testing machine. In all cases the flexural modulus obtained by three-point bending is slightly greater than that obtained by five-point bending. This fact could be related to the determination of the redundant force X, as it has not been considered the stiffness of the supports.

Moreover, in spite of values of G obtained by three-point bending and five-point bending agree, they differ with respect to those obtained in Table 3. The discrepancy in G results could be related to the stiffness of the system.

The regression coefficients in the case of five-point bending are greater than in the case of three-point bending. Otherwise it is noticeable the fact that small changes in the values of k_s and k_1 affect mainly in the result of G but not in the coefficient of regression in a significant manner.

Calculations have been carried out with all the correction terms. Table 5 shows the flexural modulus obtained by both methods, determined with correction terms and without correction terms. It can be seen that in the case of five-point bending the difference is negligible in all cases, due to the small rotated angles at the ends. In the case of three-point bending, uncorrected values are 3% greater than corrected ones.

Table 5. Differences between flexural moduli obtained with corrections and without corrections

	S1		S2		S3	
E_f (MPa)	3P	5P	3P	5P	3P	5P
Corrected	105.7	104.3	103.5	101.8	104.6	102.5
Uncorrected	108.5	104.4	106.2	101.9	107.4	102.6

Fig. 23 shows experimental and regression moduli obtained in three-point and five-point bending. In the case of three-point bending the values corresponding to span 200 mm have not been included in the figure. The variation range of five-point modulus values E_{5p} is greater than that of three-point modulus values E_{3p}. This fact could explain the better values of R^2 obtained in the case of five-point bending.

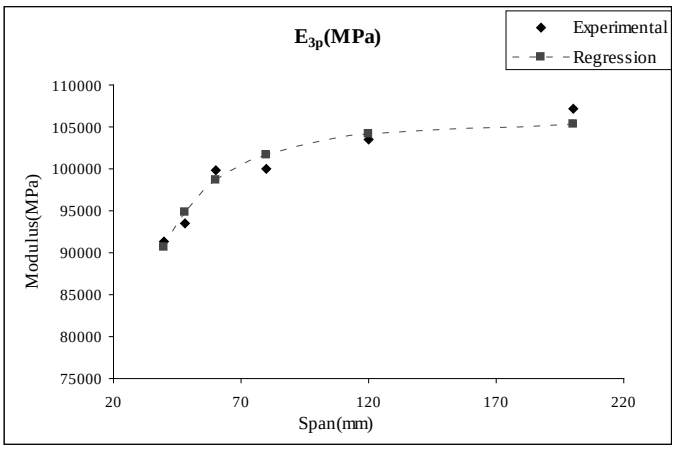

(a)

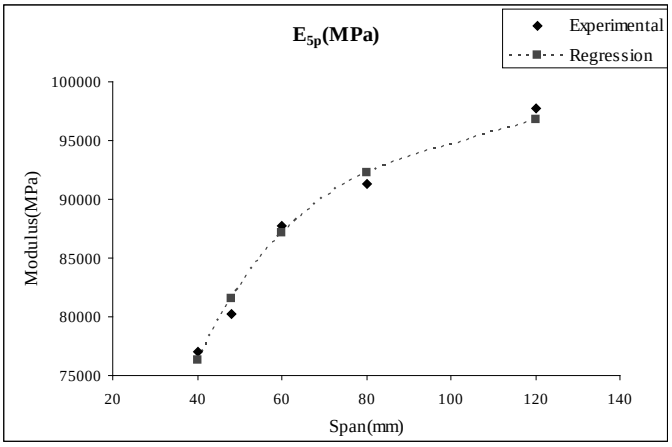

(b)

Fig. 23. Experimental and regression moduli: a/ Three-point bending; b/ Five-point bending

CONCLUSIONS

A novel two-sense support system designed and manufactured in Ikerlan has been used for defining a five-point bending test. Flexural modulus and out-of plane shear modulus obtained with the novel supports in three-point and five-point bending tests agree reasonably with those obtained with a standard three point fixture in other testing machine. Moreover, the correlation coefficients of the linear regression in the case of five-point bending are better than in the case of three-point bending. Otherwise, the correction factors related to the variation of contact point between specimen and supports have more influence in the case of three-point bending than in five-point bending. This is due to the fact that the partial clamping in five-point bending reduces the bending angles at the ends.

The results obtained depend in a great extent on the stiffness of the system. It would be desirable to increase the stiffness of the bidirectional supports in the next version of the supports.

Two-sense five-point bending is a promising test method for fatigue tests, as stresses of both signs can be obtained at the same point. Thus, after having checked the suitability of the analytic model of the five-point bending test, it can be applied to fatigue cases. The advantage with respect to three-point bending is that the stress is much greater for a given displacement. This reasoning is extensible also for obtaining the longitudinal strength of unidirectional composites in the regime of small displacements. Otherwise,the test configuration and model proposed is valid for any orthotropic material.

REFERENCES

1 W. Van Paepegem y J. Degrieck, Experimental set-up for and numerical modelling of bending fatigue experiments on plain woven glass/epoxy composites, *Composite Structures*, **51** (2001) 1-8.
2 I. De Baere, Design of a three- and four-point bending setup for fatigue testing of fibre-reinforced thermoplastics, Gent University (UGent), Gent, Belgium, 2005.
3 I. de Baere, J. Van Paepegem, J. Degrieck J, Comparison of different setups for fatigue testing of thin composite laminates in bending, *International Journal of Fatigue*, **31** (2009) 1095-1101.

4 W.C. Kin, K.H. Dharan, Analysis of five-point bending for determination of the interlaminar shear strength of unidirectional composite materials, *Composite Structures*, **30** (1995) 241-251
5 F. Mujika, On the difference between flexural moduli obtained by three-point and four-point bending tests, Polymer Testing 25(2006) 214-220.
6 F. Mujika, On the effect of shear and local deformation in three-point bending tests, *Polymer Testing* **26** (2007) 869–877.
7 ISO 14125:1998, Fibre-reinforced Plastic Composites, Determination of Flexural Properties, 1998.